

Synthesis, characterization and dioxygen reactivity of copper(I) complexes with glycoligands†‡

Ziad Damaj,^a Federico Cisnetti,^c Laurent Dupont,^a Eric Henon,^d Clotilde Policar^{*c} and Emmanuel Guillon^{*a,b}

Received 21st January 2008, Accepted 28th March 2008

First published as an Advance Article on the web 7th May 2008

DOI: 10.1039/b801109e

A new family of copper(I) complexes with “glycoligands” containing a central saccharide scaffold, with 2-picolyl ether groups or 2-picolylamine or *N*-imidazolylamine groups, has been prepared and characterized. For this purpose, the following tetradentate ligands have been synthesized: methyl 2,3-di-*O*-(2-picolyl)- α -D-lyxofuranoside (**L1**), 1,5-anhydro-2-deoxy-3,4-di-*O*-(2-picolyl)-D-galactitol (**L2**), 5-(amino-*N*-(2-salicyl))-5-deoxy-1,2-*O*-isopropylidene-3-*O*-(2-picolyl)- α -D-xylofuranose (**L3**), and 5-(amino-*N*-(2-salicyl))-5-deoxy-1,2-*O*-isopropylidene-3-*O*-(methylimidazol-2-yl)- α -D-xylofuranose (**L4**). The ligands and the complexes were characterized by elemental analysis, IR, ¹H and ¹³C NMR spectroscopies, ESI mass spectrometry, and cyclic voltammetry. Collaterally with the experimental work, HF-DFT(B3LYP/6–31G*) computations were performed to obtain additional structural information. The Cu(I) complexes are found to be pentacoordinated. The redox properties and the O₂-reactivity of the Cu^I**L_n** complexes have been studied. Reactions of Cu(I) complexes with dioxygen in ethanol yield stable Cu(II) complexes as confirmed by UV-visible spectrophotometry and EPR spectroscopy.

Introduction

Investigations of the reactivity of copper(I) complexes with molecular dioxygen is a worthy endeavour from the point of view of understanding of the active intermediate species involved in copper–protein O₂ binding/activation and for “green” practical reagents or catalysts for substrate oxidations. The reactions of Cu(I) complexes with O₂ and the oxidative properties of the resulting Cu/O₂ complexes have attracted much interest during the past decades because of their potential relevance to biochemical systems^{1,2} and synthetic catalysis.^{3,4} A great deal of knowledge has been obtained from these studies and a number of structural and reactivity types are now well established.^{5–7}

Another way of application of such complexes is the packaging industry. Indeed, copper(I) complexes can be used as oxygen scavenger. Oxygen scavenging is part of “active packaging”, which

refers to positive package/product/environment interaction. This is one of the most innovative and promising areas, in recent years, in packaging in general and in food packaging in particular. In active packaging the product, the package and the environment interact in a positive way, resulting in either an extension of the product's shelf-life or the attainment of some specific property that cannot be obtained by other means. Such interactions are beneficial and are therefore sought after.⁸ Many products are sensitive to oxygen and deteriorate in its presence. Modified atmosphere packaging (MAP) of foods, developed about two decades ago, is capable of providing, in some cases, a partial solution to this problem. In MAP, air is replaced by a mixture of gases (N₂, CO₂, and small amount of O₂) at partial pressures different from that of air. For many foods, the levels of residual oxygen that can be achieved by regular MAP technologies are too high for maintaining the desired quality and for achieving the sought shelf-life. Oxygen scavengers are capable of reducing the oxygen concentration in a package to very low levels. Most of the commercially available oxygen scavengers contain iron as the oxygen absorber and are marketed in the form of a sachet. They require water to activate them.⁸ Recently, oxygen-scavenging films have been developed as well. Some of these films contain iron in their structure, while others are based on organic compounds that absorb oxygen after being activated, normally by ultra-violet light.^{9–11}

Keeping this aim in mind we propose to develop a new family of oxygen scavengers based on copper(I) complexes with ligands derived from natural molecules. These complexes will be then incorporated in organic polymer. Some of us have recently initiated a novel strategy using saccharides as central scaffolds to generate ligands for transition metal cations (named glycoligands).^{12–15} This “glycoligand strategy” is original in that it uses sugars as a distribution frame to generate a polydentate chelating claw

^aInstitut de Chimie Moléculaire de Reims, Equipe Chimie de Coordination, Université de Reims Champagne-Ardenne, UMR CNRS 6229, Faculté des Sciences, B.P. 1039, F-51687, Reims cedex 2, France. E-mail: emmanuel.guillon@univ-reims.fr; Fax: +33 (0)3 26 91 32 43

^bESIEC (Ecole Supérieure d'Ingénieurs en Emballage et Conditionnement), Pôle Technologique Henri Farman, B.P. 1029, F-51686, Reims cedex 2, France

^cInstitut de Chimie Moléculaire et des Matériaux d'Orsay, Equipe de Chimie Bio-organique et Bio-inorganique, Université Paris-Sud 11, UMR CNRS 8182, F-91405, Orsay cedex, France. E-mail: cpolicar@icmo.u-psud.fr; Fax: +33 (0)1 69 15 72 81

^dInstitut de Chimie Moléculaire de Reims, Equipe BSMA, Université de Reims Champagne-Ardenne, UMR CNRS 6229, Faculté des Sciences, B.P. 1039, F-51687, Reims cedex 2, France. E-mail: eric.henon@univ-riems.fr; Fax: +33 (0)3 26 91 84 97

† Z. D., F. C. and C. P. for ligand design and synthesis; Z. D., L. D. and E. G. for synthesis of the complexes and physico-chemical studies.

‡ Electronic supplementary information (ESI) available: Fig. S1, S2, S3, ZPE corrected potential energies and Cartesian coordinates of all minima obtained within the water PCM model. See DOI: 10.1039/b801109e

for transition metal cations. The glycoligands show interesting characteristics, such as a fine-tuning of the geometry at the metal centre, which is stereogenic.^{13,14}

In this paper, we report the synthesis, characterization, and oxygenation reactivities of Cu(I) complexes with such glycoligands. A computational approach helped us to examine the structure of the complexes. The coordination structure shows two five-membered chelate rings or one five- and one six-membered chelate rings fused by the furanoside or the pyranoside framework. A discussion about the influence of the various substituents on the saccharide scaffold on the redox properties and on the dioxygen reactivity is provided.

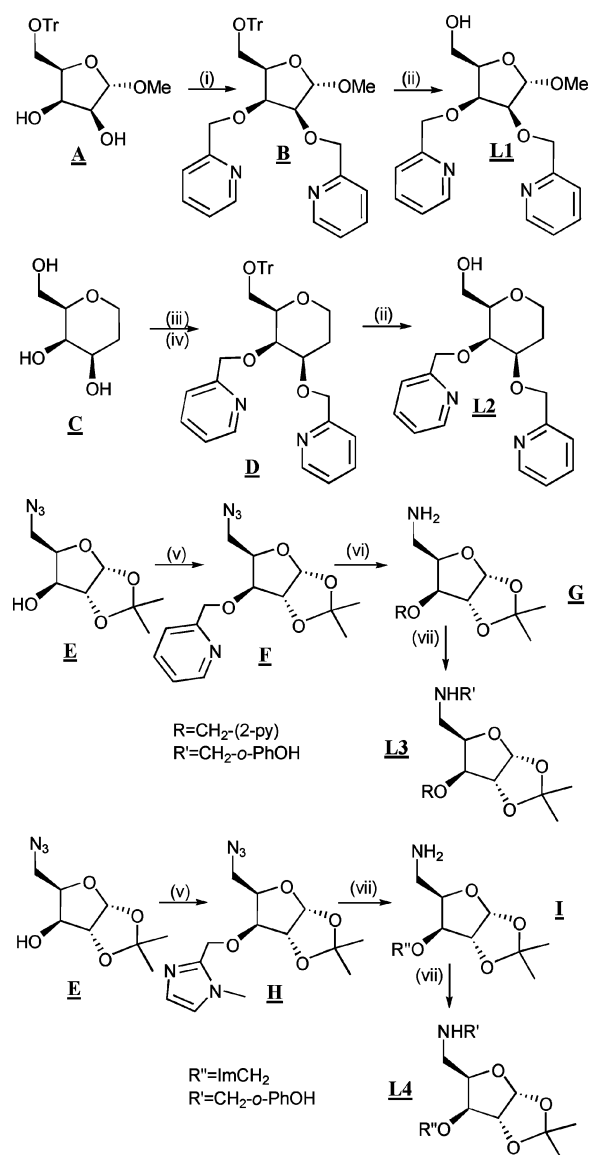
Results and discussion

Synthesis of the glycoligands

Four glycoligands have been synthesized (see Scheme 1). Here are presented two glycoligands of *first generation* (*viz.* **L1** and **L2**), derived from monosaccharides by simple alkylation of selected hydroxyl groups by Lewis bases such as pyridine. Efficient alkylation phase transfer protocols derived from a benzylation protocol,¹⁶ have been used. Two sets of conditions are described: a liquid–liquid phase transfer toluene/water and a liquid–solid toluene/DMSO¹³ phase transfer. These first-generation glycoligands are characterized by a chelating unit involving 2-picoly ether groups.^{12–15} In order to improve binding strength with metal cations, a *second generation* of glycoligands have been designed, that involve amine groups instead of ether groups (see Scheme 1, **L3**, **L4**). In order to do so, the *xylo* azido-alcohol **E**¹⁷ was alkylated using a liquid–liquid phase transfer protocol. The azide was then reduced. Functionalization of the amine function was achieved by reductive amination. The synthetic pathways are described in Scheme 1.

Synthesis and characterization of Cu(I) complexes

The copper(I) complexes were readily prepared by mixing a copper(I) salt ($\text{Cu}(\text{CH}_3\text{CN})_4(\text{PF}_6)$) methanolic solution with an equimolar amount of the glycoligand in the same solvent under anaerobic conditions. These Cu(I) complexes are very air-sensitive, and in ethanolic solution they are rapidly oxidized to Cu(II) complexes upon exposure to air at room temperature. The complexes were isolated as colourless microcrystalline solids for $\text{Cu}^{\text{I}}\mathbf{L1}$ and $\text{Cu}^{\text{I}}\mathbf{L2}$, and as oils for $\text{Cu}^{\text{I}}\mathbf{L3}$ and $\text{Cu}^{\text{I}}\mathbf{L4}$ in good yield (higher than 90%). As the complexes were extremely sensitive to air, it was necessary to handle them in a glove box. The Cu(I) complexes were soluble in polar organic solvents such as ethanol or acetonitrile. Each complex has been characterized by elemental analysis, IR spectroscopy, mass spectrometry, and cyclic voltammetry. Unfortunately, all attempts to obtain well-formed crystals suitable for X-ray determination have failed. The IR spectra of the complexes are consistent with the presence of coordinated picolyl ($\nu_{\text{C=N}}$ at 1615 cm^{-1}).¹² Satisfactory elemental analysis and mass spectra were obtained for all the complexes, which confirm the formation of 1 : 1 complexes (metal to ligand ratio) consistent with monocationic $[\text{Cu}^{\text{I}}\mathbf{Ln}(\text{H}_2\text{O})]^+\text{PF}_6^-$ species (**Ln** corresponds to the ligand in its neutral form, *i.e.* with the phenol moiety protonated in the case of **L3** and **L4**). These data



Scheme 1 Synthetic pathways for **Ln**. *Reagents and conditions:* **L1**: (i) Picolylation protocol 1: 2-picoly chloride hydrochloride, toluene/ NaOH_{aq} 50%, NBu_4HSO_4 , *tert*-amyl alcohol, overnight; (ii) HCl_{aq} , EtOH, overnight. **L2**: (iii) TrCl , py, DMAP, 50 °C, overnight; (iv) picolylation protocol 2: 2-picoly chloride, DMSO–toluene, *tert*-amyl alcohol, $\text{NaOH}/\text{K}_2\text{CO}_3$, overnight. **L3/L4**: (v) alkylation protocol 1: 2-picoly chloride hydrochloride or methyl(*N*-methylimidazol-2-yl) chloride hydrochloride, toluene/ NaOH_{aq} 50%, NBu_4HSO_4 , *tert*-amyl alcohol, overnight; (vi) MeOH, Pd/C, H_2 (5 bar), 3h (vii) salicylaldehyde, EtOH, NaBH_4 , 0 °C, 30 min.

allowed us to propose a five-coordinated copper(I) ion with one oxygen atom from a water molecule and the nitrogen and oxygen atoms of the two picolyl moieties for $\text{Cu}^{\text{I}}\mathbf{L1}$ and $\text{Cu}^{\text{I}}\mathbf{L2}$. For $\text{Cu}^{\text{I}}\mathbf{L3}$ and $\text{Cu}^{\text{I}}\mathbf{L4}$, the phenolic oxygen atom, maybe involved in the coordination, is protonated as underlined on the UV-visible spectra (Fig. 1), which do not present any phenolate specific transition around 400–450 nm. The deprotonation of the phenolic group was underlined by the addition of an equimolar of strong base on the two complexes $\text{Cu}^{\text{I}}\mathbf{L3}$ and $\text{Cu}^{\text{I}}\mathbf{L4}$, which leads to the formation of $\text{Cu}^{\text{I}}\mathbf{LH}_{-1}$ species. The $\pi \rightarrow \pi^*$ transition

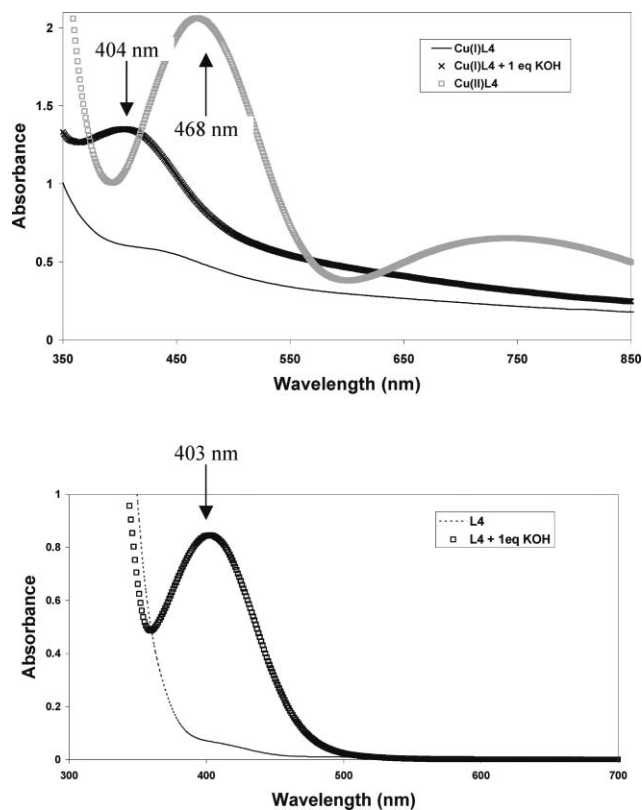


Fig. 1 UV-visible spectra in aqueous solution of $\text{Cu}^{\text{I}}\text{L4}$ and L4 , 3.70 mM, underlining the absorption transition of the phenolate moiety in presence of an equivalent of strong base.

corresponding to the phenolate moiety was detected at 404 nm (Fig. 1, top). This phenomenon is also confirmed by the UV-visible spectra of the ligand alone (Fig. 1, bottom). Indeed, the ligand spectrum shows the appearance of the $\pi \rightarrow \pi^*$ phenolate transition at 403 nm in presence of an equivalent of strong base.

DFT calculations

In parallel with the experimental work, we performed DFT molecular orbital computations to obtain further information about the structure of the complexes. The details of the quantum mechanical calculations are reported in the Experimental section. Starting from a pentacoordinate environment (suggested by our experimental results) with a water molecule occupying an apical position, each geometry was first optimized within the gas-phase model. Solvent effects on the structures were subsequently assessed by the water solvent polarized continuum model^{18–20} (PCM) (see computational details in the Experimental section). Comparison with the gas-phase results indicates that the non-specific interaction of the solvent exerts no substantial effect on the geometrical parameters of all complexes. The PCM results are presented.

The solvent-optimized geometries of $\text{Cu}^{\text{I}}\text{L1}$ and $\text{Cu}^{\text{I}}\text{L2}$ are shown in Fig. 2. For these two complexes, the computational study aims to get an insight into the structures involving a five-coordinate copper atom. Both complexes are found to adopt a very similar distorted square pyramidal geometry. The Cu–N distances are in the range 1.920–1.938 Å while the Cu–O distances are predicted

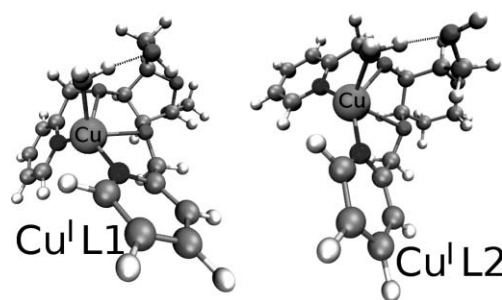


Fig. 2 Pentacoordinate distorted square pyramidal structures for $\text{Cu}^{\text{I}}\text{L1}$ and $\text{Cu}^{\text{I}}\text{L2}$; HF-DFT (B3LYP/6-31G*/PCM) optimized geometries.

to range from 2.112 to 2.511 Å. In both cases, the two distances from the copper(i) ion to the O atoms of the glycoligand are substantially different (by 0.09–0.16 Å for $\text{Cu}^{\text{I}}\text{L1}$ and $\text{Cu}^{\text{I}}\text{L2}$, respectively) reflecting an asymmetry of the copper bonding environment around the sugar. The main difference between these two copper(i) complexes is that they exhibit this asymmetry with an opposite sign. Due to the conformational freedom of the hydroxyl group a short hydrogen-bond ($\text{H} \cdots \text{O}$ distance 1.767–1.789 Å for $\text{Cu}^{\text{I}}\text{L1}$ and $\text{Cu}^{\text{I}}\text{L2}$, respectively) is formed with the water molecule. Non hydrogen-bridged conformers have also been found, with slightly higher energies.

Concerning the $\text{Cu}^{\text{I}}\text{L3}$ and $\text{Cu}^{\text{I}}\text{L4}$ complexes, in the absence of X-ray determination, the question was whether the hydroxyl of the phenol moiety could interact with the metal ion. That is the reason why the oxygen atom was placed around the copper ion before starting the geometry optimizations. The resulting bond distances and angles about the copper center are consistent with a pentacoordinate distorted square-pyramidal structure (Fig. 3) involving the protonated phenolic oxygen atom. However, the Cu–O bond distance (involving the phenolic oxygen atom) in $\text{Cu}^{\text{I}}\text{L3}$ (2.875 Å) significantly differs from that found in $\text{Cu}^{\text{I}}\text{L4}$ (2.567 Å). Internal rotations of the phenol ring were then performed to move the hydroxyl group away from the metal center in the $\text{Cu}^{\text{I}}\text{L3}$ complex. Another minimum, of slightly higher energy (by about 0.5 kcal mol⁻¹), was then found, which underlines that the interaction between the phenolic oxygen atom and the copper(i) ion is relatively weak in the present $\text{Cu}^{\text{I}}\text{L3}$ complex. The Cu–N distances (1.896–2.019 Å) in $\text{Cu}^{\text{I}}\text{L3}$ are very similar to those in $\text{Cu}^{\text{I}}\text{L4}$ complex (1.893–2.041 Å), while the distances between the copper(i) ion and the sugar oxygen atom are significantly different for $\text{Cu}^{\text{I}}\text{L3}$ (2.216 Å) and $\text{Cu}^{\text{I}}\text{L4}$ (2.384 Å). It is to be noticed that hydrogen bonding (1.888 and 1.860 Å for $\text{Cu}^{\text{I}}\text{L3}$ and $\text{Cu}^{\text{I}}\text{L4}$, respectively) is predicted between the water molecule

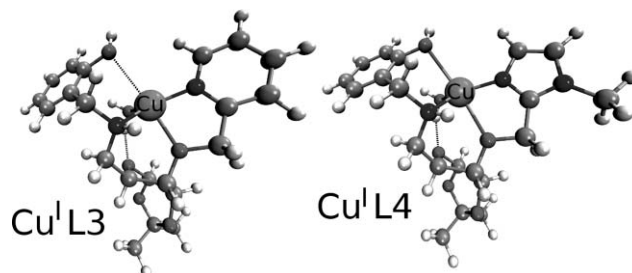


Fig. 3 Pentacoordinate distorted square pyramidal structures for $\text{Cu}^{\text{I}}\text{L3}$ and $\text{Cu}^{\text{I}}\text{L4}$; HF-DFT (B3LYP/6-31G*/PCM) optimized geometries.

and the ring oxygen atom as depicted Fig. 3. The distance between the copper(i) ion and the apical water oxygen atom is very similar (about 2.09 Å) than that found in Cu^IL1 and Cu^IL2 complexes (about 2.12 Å). All these results favourably agree with the experimentally suggested five-coordinate copper center. However, other coordination arrangements cannot be rigorously ruled out. As above-mentioned, the starting geometries used for the optimization of Cu^IL3 and Cu^IL4 were chosen within a pentacoordinate copper surrounding, which involves the phenolic oxygen atom. Supplementary calculations using other initial guess geometries suggest that copper might tend to adopt a distorted tetrahedral geometry of higher energy (as shown in Fig. S1, ESI[†]). But there is only small energetic differences between these geometries and the presented pentacoordinate structures (< 0.5 kcal mol⁻¹ at the B3LYP/6-31G* level of theory including zero-point vibrational energy correction). On the other hand, optimizations starting from the above presented five-coordinated geometries (Fig. 3) and interchanging the moiety phenol with a water molecule at the apical position (this can be achieved because the phenol chelating group possesses internal rotational degrees of freedom) lead to new minima about 6 kcal mol⁻¹ higher in energy (see Fig. S2, ESI[†]).

Electrochemistry

The redox potential is a key point in the electronic transfer processes. It notably depends on the electronic properties of the ligands. Thus, the electrochemical behaviours of the complexes were studied by cyclic voltammetry (Fig. 4). All potentials were measured in acetonitrile with tetrabutylammonium hexafluorophosphate as the supporting electrolyte and internally referenced to the ferrocenium/ferrocene redox couple. Potentials were reported vs. the Fc⁺/Fc couple.²¹ The cyclic voltammogram revealed an electrochemically irreversible oxidation of the Cu(i) complexes (Table 1), which could be assigned to the Cu^{II}L_n-Cu^IL_n

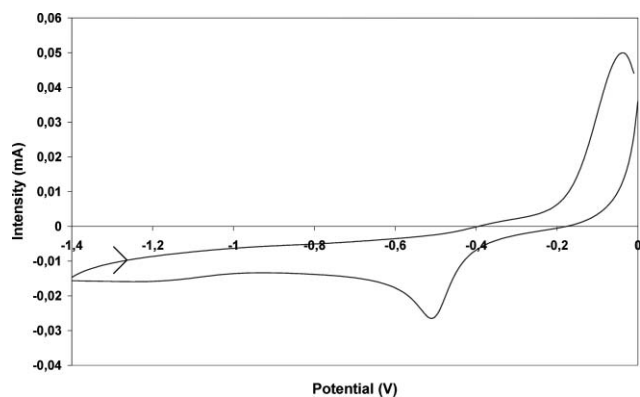


Fig. 4 Cyclic voltammogram of complex Cu^IL3, 10⁻³ mol L⁻¹, in CH₃CN containing 0.10 mol L⁻¹ [n-Bu₄N][PF₆] at a scan rate of 100 mV s⁻¹.

Table 1 Results from cyclic voltammetry experiments on solutions of Cu(i) complexes

	CuL1	CuL2	CuL3	CuL4
E_{pa}^a/V (vs. Fc ^{+/0})	-0.40	-0.18	-0.57	-0.64

^a According to Fc^{+/0} = 0.40 V vs. SCE.¹⁸

couples. The oxidation potential values, which follow the order: Cu^IL4 < Cu^IL3 < Cu^IL1 < Cu^IL2, are in agreement with the increasing electron-withdrawing effect of the ligands. Indeed, the more electron rich copper(i) complexes with better donor ligands are easier to oxidize than those with electron-deficient ligands.²² Turning to using the results of our theoretical study, we consider the highest occupied molecular orbital (HOMO) energy, since it is clear that this property should be physically correlated with oxidation potential.

While Koopmans theorem (the first ionization energy of a molecule is equal to the energy of the HOMO) does not apply to DFT HOMO eigenvalues or to orbital eigenvalues from a solvated wave function, they can still often be correlated with ionization potentials.²³ The negative HOMO energies (eV) found at the B3LYP/6-31G*/PCM level of theory for L4, L3, L1 and L2 are 4.60, 5.02, 5.40 and 5.39, respectively. This relative order is preserved when doing a single point energy calculation at the B3LYP/6-311G** level of theory. According to this reasonable qualitative theoretical approach, the ionization potentials of L3 and L4 should be the smallest ones, supporting the experimental findings. Further analysis would require more accurate predicting methods of redox potential (accounting for the thermal and the aqueous free energy of solvation contributions). Moreover, such an electrochemical behaviour (electrochemically irreversible waves) is difficult to interpret and hinders a more detailed comparison between the electronic properties of the complexes.

Dioxygen reactivity

We have investigated the reactivity of the copper(i) complexes towards dioxygen in some detail. These experiments were performed in ethanolic solution and were monitored using electronic absorption and EPR spectroscopies, and ESI-mass spectrometry. The presence of dioxygen in solution resulted in an apparent colour change from light yellow to a more or less dark green, which indicates that dioxygen reacts with copper(i) species to lead to a copper(ii) species. The absorption spectral change in the reaction of the Cu(i) complexes with dioxygen is shown in Fig. 5. The oxidation process leads to a hyperchromic phenomenon with an increase of the absorbance. These dark green Cu(ii) species showed a single intense broad d-d band in the visible region close to 720 nm (717 (ε = 126), 704 (ε = 149), 709 (ε = 264), 742 nm (ε = 176 mol⁻¹ dm³ cm⁻¹), corresponding to Cu^{II}L1, Cu^{II}L2, Cu^{II}L3

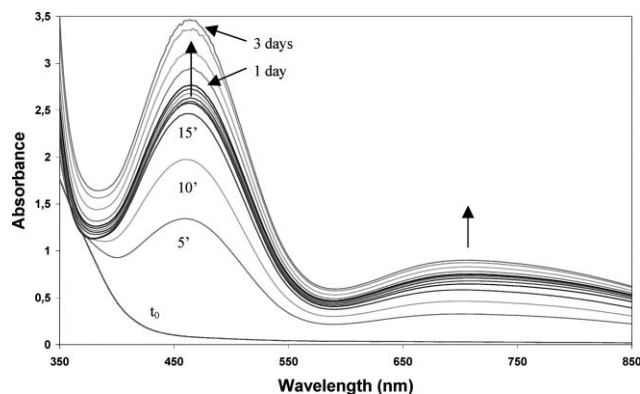
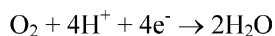
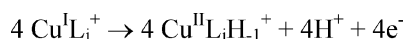


Fig. 5 Development of optical absorption spectra of Cu^IL3, 3.41 mM, upon oxygenation in ethanolic solution at room temperature.

and Cu^{II}L4, respectively). In the case of Cu^{II}L3 and Cu^{II}L4 a band around 460–470 nm appears, which is assigned to a phenolate to Cu(II) ligand-to-metal charge transfer (LMCT).²⁴ The transition around 720 nm (*e.g.* $\sim 14\,000\text{ cm}^{-1}$), that is unsymmetrical, is consistent with a tetragonal distorted octahedral geometry with a CuN₂O₄ chromophore²⁵ and confirms the formation of Cu(II) species.

Moreover, the increase of the transition at 468 nm (Fig. 5), assigned to the LMCT transition of the Cu(II)–phenolate chromophore, indicates that the oxidation process leads to the deprotonation of the phenol moiety through an electron and proton transfer according to the Scheme 2.



Scheme 2 Proposed oxidation process ($\text{L}_i = \text{L}_3$ or L_4).

The coordination of the Cu(II) metallic cation by the phenolate moiety is confirmed by the disappearance of the $\pi \rightarrow \pi^*$ transition (404 nm) of the phenolate ion on behalf of a LMCT transition (468 nm) of the Cu(II)–phenolate chromophore (Fig. 1 top).

In order to identify the chemical species present in solutions of the oxygenated copper complex species, ESI-MS spectra were recorded. The spectra revealed positive ions at m/z values corresponding to $[\text{Cu}^{\text{II}}\text{L}_i]$ species. This is consistent with the fact that the dioxygen was not fixed on the copper(II) complexes, which is in contradiction with most of the publications on this topic.⁶ Nevertheless, we can not exclude the possible formation of intermediate species during the redox process, in which the dioxygen is coordinated to the complex.

Bubbling nitrogen into an oxygenated solution of copper complexes, or purging the oxygenated solution with a stream of argon gas resulted in no noticeable loss and/or change in absorption intensity of the UV-Vis spectra of the solutions. Thus, the oxygenation of the complexes was physico-chemically irreversible. Nevertheless, the addition of a small amount of sodium borohydride (NaBH_4) leads to the discoloration of the solution, which indicates that the copper(II) complexes may be reduced to the corresponding copper(I) complexes through NaBH_4 reduction. The regenerated copper(I) complex is then active towards oxygen.

The dioxygen reactivity with the Cu(I) complexes was also followed by tracing the maximum intensity of the d–d transition (extracted from Fig. 5) vs time (Fig. 6) This figure underlines two types of behaviour. Cu^IL3 and Cu^IL4 rapidly react with dioxygen to reach equilibrium after 1 and 4 h, respectively, while Cu^IL1 and Cu^IL2 exhibit a slower oxidation kinetics. Indeed, the curves present two stages. (1) a relatively fast kinetics in which more than 50% of the copper(I) was converted into copper(II) and (2) a slower kinetics leading to a plateau (corresponding to 100% of Cu(I) conversion) or a pseudo-plateau after 6 h. These curve shapes are in agreement with the potential values of the Cu(II)/Cu(I) systems. Indeed, the fact that the redox potential of Cu^IL3 and Cu^IL4 are lower than those of Cu^IL1 and Cu^IL2 (see Table 1) suggested a higher reactivity of the former towards dioxygen.⁵

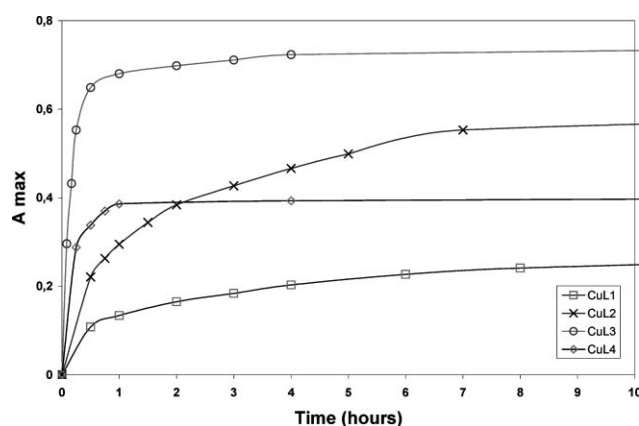


Fig. 6 Evolution of the maximal absorbance of Cu^IL_{*n*}, 3.50 mM, complexes in contact with dioxygen at $\lambda_{\text{max}} = 717, 704, 709$ and 742 nm for Cu^IL1, Cu^IL2, Cu^IL3 and Cu^IL4, respectively, as a function of time at room temperature in ethanolic solution.

EPR spectroscopy

In order to identify the chemical species present in solutions of the oxygenated copper complexes, EPR spectra of the solutions were recorded. Fig. 7 shows as example the 77 K EPR spectrum of the green solution recorded after the reaction of O₂ with Cu^IL2 in ethanol, and the spectra of the other complexes are similar. The EPR spectra display a typical anisotropic copper(II) signal with four lines in parallel region arising from the hyperfine coupling of the $S = 1/2$ electron spin of Cu(II) with its nuclear spin $I = 3/2$. These spectra reveal that the Cu(II) center is axial ($g_{\parallel} > g_{\perp} > 2.0$), with simulated spin-Hamiltonian parameters reported in Table 2.

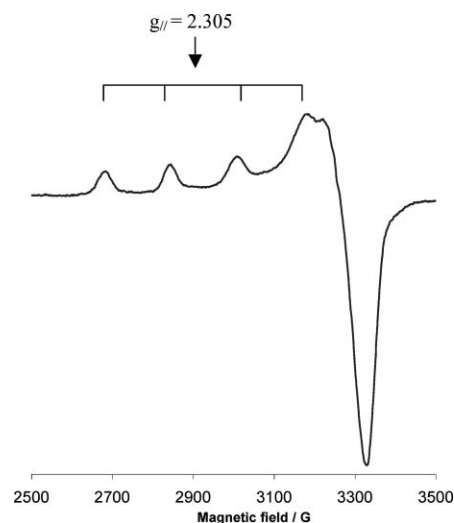


Fig. 7 77 K EPR spectrum of Cu^IL2, 4.24 mM, complex generated by oxygenation of Cu^IL2 in ethanol at 293 K.

These values lie in the middle of the Peisach and Blumberg maps²⁶ and most closely correlate with copper in the +2 oxidation state in tetragonal CuN₂O₄ structures ($g_{\parallel} \sim 2.28, A_{\parallel} \sim (150\text{--}180) \times 10^{-4}\text{ cm}^{-1}$).²⁷ The spin-Hamiltonian parameters are in agreement with a tetragonal elongation of the octahedron.^{28,29} Indeed, if an axial coordination around copper(II) ion exists, the $d_{x^2-y^2}$ orbital receives an increase in destabilization (*i.e.* $\Delta E(x^2 - y^2 \rightarrow xy)$

Table 2 EPR parameters of copper(II) complexes in ethanolic solution

	g_{\parallel}	g_{\perp}	$10^{-4}A_{\parallel}/\text{cm}^{-1}$
Cu ^{II} L1 ^a	2.297	2.075	178.0
Cu ^{II} L2 ^a	2.305	2.066	179.7
Cu ^{II} L3 ^a	2.273	2.080	147.5
Cu ^{II} L4 ^a	2.268	2.071	173.0

^a Values obtained by simulation.

increase), which causes an increase in the g value as can be seen from eqn (1) and (2):

$$g_{\parallel} = g_e - \frac{8\lambda}{\Delta E(x^2 - y^2 \rightarrow xy)} \quad (1)$$

$$g_{\perp} = g_e - \frac{2\lambda}{\Delta E(x^2 - y^2 \rightarrow xz, yz)} \quad (2)$$

where λ represents the spin-orbit coupling constant, ΔE is the difference in the corresponding state energies, and g_e the g factor of the free electron.

In addition, the value of the ratio $g_{\parallel}/A_{\parallel}$, which is approximately equal to 130 cm (except for Cu^{II}L3, $g_{\parallel}/A_{\parallel} = 154$ cm), suggests an absence of significant dihedral angle distortion in the xy -plane.²⁶ This conclusion is supported by the EPR parameters of tetrahedral complexes, for which $g_{\parallel}/A_{\parallel}$ is greater than 180 cm.³⁰

We have also examined the deprotonated Cu^{II}L n structures using DFT molecular orbital computations in order to confirm the proposed geometries. First, five-coordinate structures analogous to that found for copper(I) complexes were obtained (see Fig. S3, ESI[†]). In these molecules, the phenolate oxygen atom is now strongly coordinated to the metal ion (about 1.87 Å). However, additional geometries have been found with structural features more consistent with a six-coordinated tetragonal environment (Fig. 8) involving the sugar ring oxygen atom. These structures have nearly the same energy (less stable by only 1 kcal mol⁻¹) than their pentacoordinate counterpart. They are the analogous of those obtained for copper(I) by interchanging the phenol moiety with a water molecule at the apical position (see Fig. S2, ESI[†]). In the absence of hydrogen bonding between the ring oxygen atom and the phenolic hydroxyl hydrogen, the ring oxygen atom gets closer to the metal ion. The distance between copper and this oxygen atom is not so large (2.642 and 2.542 Å for Cu^{II}L3 and Cu^{II}L4, respectively) to rule out possible interactions. Indeed, the

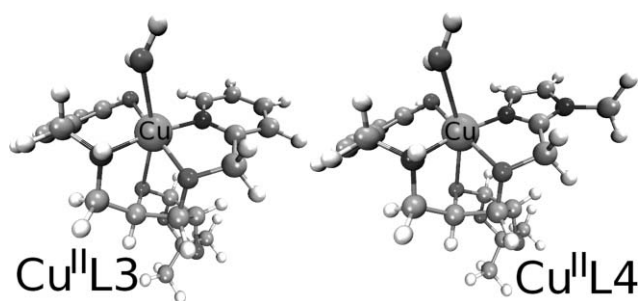


Fig. 8 Six-coordination tetragonal (distorted octahedral) structures for Cu^{II}L3 and Cu^{II}L4; HF-DFT (B3LYP/6-31G*/PCM) optimized geometries.

wave function displays some contributions of the ring oxygen atom lone pair orbital to molecular orbitals involving copper 3d functions. Thus, hexacoordinate complexes with a slightly distorted octahedral geometry are also predicted for Cu^{II}L3 and Cu^{II}L4. Comparison with the gas-phase results indicates that the non-specific interaction of the solvent exerts no substantial effect on the geometrical parameters of all complexes.

Conclusions

We have synthesized four copper(I) complexes with tetradentate glycoligands. These complexes have been isolated and fully characterized. Thus, based on the chemical and spectroscopic evidence, the structures of CuL n are best described as pentacoordinate, probably square-pyramidal, and six-coordinate tetragonal Cu(I) and Cu(II) complexes, respectively. The results of the computational investigation give theoretical support to the existence of these structures. In all these species, the Cu(I) ion is coordinated to two nitrogen and two oxygen atoms from the glycoligands, the coordination sphere being completed with one water molecule.

In solution, these four compounds behave quite differently. Cu^IL1 and Cu^IL2, which have higher redox potential values, react more slowly with dioxygen. On the other hand, Cu^IL3 and Cu^IL4 react rapidly with dioxygen in accordance with their lowest redox potential values. These results of the reactivity towards dioxygen of the Cu(I) complexes are promising for future application in the packaging field.

Future studies of incorporation of these complexes into organic polymers and on their reactivity with O₂ may further contribute to our understanding of oxygen scavenger processes. Indeed, data on absorption capacity of oxygen scavengers and the absorption rate are required for designing an optimal and cost-effective package using a scavenger. The capacity and rate of scavenging of copper(I)-based oxygen scavenger depend also on the environment inside the package, especially if carbon dioxide is present. The information provided by oxygen scavenger manufacturers does not always provide all the information needed for designing a good package. Much more insight into the action of oxygen scavengers in different environments is required.

Experimental

Materials

All the solvents were purified by conventional procedures, distilled and deaerated prior to use. Solutions of the copper(I) salt (Cu(CH₃CN)₄(PF₆)) and complexes were handled under inert atmosphere in a glove box. All the chemicals which were commercially available (Aldrich or Acros) were used as supplied.

Analytical procedures

Elemental analyses (C, H and N) were carried out on a Perkin-Elmer 2400 C, H, and N elemental analyzer. The copper analyses were performed on an ICP-AES Liberty Series II Varian apparatus. The IR spectra were recorded from KBr pellets on a Nicolet Avatar 320. ¹H and ¹³C{¹H} NMR spectra were recorded at room temperature on a Bruker AV360 spectrometer in CDCl₃. ESI-MS were recorded on a Finnigan Mat 95S in a BE configuration at low resolution out on a hybrid tandem quadrupole/time-of-flight

(Q-TOF) instrument, equipped with a pneumatically assisted electrospray (Z-spray) ion source (Micromass, Manchester, UK) operated in positive mode. The electrospray potential was set to 3 kV in positive ion mode and the extraction cone voltage was usually varied between 30 and 90 V in order to obtain optimized mass spectra. The solutions of complexes were introduced using a syringe pump with a flow rate of 5 $\mu\text{L min}^{-1}$. The peaks related to the complex species were identified by analyzing their specific isotopic profile due the different Cu isotopes (e.g. ^{63}Cu and ^{65}Cu). The stoichiometries of the molecular associations were determined in accordance with the higher intensity isotopic peak (e.g. ^{63}Cu). The difference between experimental and calculated m/z values was less than or equal to 0.1 unit. Complementary high resolution mass spectra (HRMS) were obtained on a Q-TOF Micromass positive ESI (CV = 30 V). The UV-Vis spectra in ethanolic solution were recorded on a Shimadzu UV-2401-PC spectrophotometer equipped with a temperature-controlled cell holder TCC-240A. The reactivity of the Cu(I) complexes towards dioxygen, followed by UV-Vis spectroscopy, was studied at room temperature in ethanolic solutions in air condition. The dioxygen comes from the naturally oxygen dissolved at atmospheric pressure.

EPR spectroscopy

The anisotropic X-band (9.44 GHz) EPR spectra of frozen ethanolic solutions were recorded at 77 K using a Bruker ESP 300 spectrophotometer. The EPR spectra were referenced to 2,2-diphenyl-1-picrylhydrazyl (DPPH) ($g = 2.0037$). All spectra were recorded using 100 kHz modulation frequency, 0.596 G modulation amplitude and microwave power of 6 mW. Simulations of EPR spectrum were performed using the WINSYMPHONIA Bruker software package.

Electrochemistry

Cyclic voltammetry was carried out using an Autolab with PG-STAT12 potentiostat (ECO Chemie). The three-electrode electrochemical cell used in our studies consisted of a glassy carbon disk working electrode, a silver electrode (separated from the complex solution) reference electrode, and a platinum plate auxiliary electrode. All sample solutions (around 10^{-3} mol L^{-1}) were prepared in acetonitrile with $(^n\text{Bu}_4\text{N})(\text{PF}_6)$ (0.10 mol L^{-1}) as the supporting electrolyte and were deaerated during 10 min. Chemical potentials were internally referenced to the $\text{FeCp}_2^+/\text{FeCp}_2$ redox couple.

Computational details

Calculations were performed using the Gaussian 03 package.³¹ Density functional theory (DFT) has become a popular choice for quantum chemical calculations on transition metal complexes. The structure of copper complexes has suitably been obtained in previous studies^{32–34} using the methodology HF-DFT with the B3LYP hybrid functional and the double-zeta 6-31G basis set family. In our study, the structures were fully optimized at the HF-DFT (B3LYP)^{35–38} level of theory using the analytical gradients and the all-electrons 6-31G* basis set (thus, adding one set of d polarization functions on the carbon, oxygen and nitrogen atoms, and one set of f polarization functions on copper atom). The unrestricted approach was used for the Cu(II) complexes. The

resulting spin contamination of the HF-DFT wave functions was very small ($S^2 = 0.7525$). For reasons of computational cost, a diffuse function could not be added for these radical species to describe the excess electron on the deprotonated oxygen atom. The minima were first optimized in the gas-phase model. As the synthesis and characterizations of the ligands and complexes were carried out using a variety of solvents (water, methanol, ethanol, and acetonitrile with a supporting electrolyte) we have chosen to estimate solvent effects on structures (full optimization) within the polarized continuum model (PCM) in the field of water (the used solvent having the largest dielectric constant, thus the largest expected effect on the structures within the PCM model). The solvent accessible surface (SAS) was employed. Comparison with the gas-phase results indicates that there is no significant solvent effect on the structures. Vibrational frequencies were determined within the harmonic approximation both in the gas-phase model and in the PCM. All minima were characterized by no imaginary frequencies. All the figures were drawn using Molden³⁹ and VMD⁴⁰ (<http://www.ks.uiuc.edu/Research/vmd/>) packages.

Synthesis

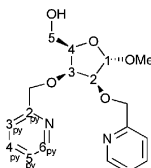
The fixation of the 2-picolyl chloride or of the 2-imidazolyl chloride was achieved using protocols derived from that published for benzylation by Szeja *et al.*¹⁶ Two general alkylation protocols were used (conditions 1 and 2 described below).

Condition 1 (solid–liquid)¹³. The alcohol derivative (*ca.* 5 mmol, 1 eq.) was dissolved in DMSO (2 mL). The organic chloride (2-picolyl chloride hydrochloride or 2-imidazolyl chloride hydrochloride) (1.2 eq. per function to be functionalized) was suspended in toluene (10 mL). Neutralisation and concomitant extraction in the toluene phase of the organic chloride were performed by pouring sat. Na_2CO_3 on this suspension until gaseous evolution ceased. The aqueous phase was decanted and the organic phase was added to the alcohol–DMSO solution. 0.1 eq. of $(\text{NBu}_4)^+(\text{HSO}_4)^-$, 0.2 mL of *tert*-amyl alcohol, and a 4 : 1 ground mixture of $\text{K}_2\text{CO}_3/\text{NaOH}$ containing a large excess of NaOH per alcoholic group to be functionalized (*ca.* 2 to 5 eq.) were added to the reaction mixture which was vigorously stirred overnight. TLC analysis (AcOEt–MeOH 9 : 1) showed in all cases the complete disappearance of the starting alcohol compound. The product was recovered by extraction (dichloromethane/water). The organic phase was dried on Na_2SO_4 and evaporated. The product was purified by column chromatography (SiO_2 , elution gradient: AcOEt to AcOEt–MeOH 9 : 1).

Condition 2 (liquid–liquid). The alcohol derivative (*ca.* 5 mmol, 1 eq.) was dissolved in toluene (14 mL). 0.35 mL of *tert*-amyl alcohol, NaOH_{aq} 50% (10 mL), $(\text{NBu}_4)^+(\text{HSO}_4)^-$ (0.1 eq.), and the organic halide (2-picolyl chloride hydrochloride or 2-imidazolyl chloride hydrochloride) (1.2 to 1.5 eq. per function to be functionalized) were added. The resulting mixture was vigorously stirred overnight, after which TLC analysis (AcOEt–MeOH 95 : 5) showed the complete disappearance of the starting alcohol. The products were recovered by extracted (dichloromethane/water). The combined organic phases were dried on Na_2SO_4 and evaporated to dryness. The product was purified by column chromatography (typically, SiO_2 , AcOEt–MeOH 95 : 5).

Methyl 2,3-di-*O*-(2-picolyl)-(6-*O*-trityl)- α -D-lyxofuranoside (B). Methyl (6-*O*-trityl)- α -D-lyxofuranoside (A) was synthesized as previously published⁴¹ and then picolylated using an adaptation of a benzylation protocol by Szeja *et al.* (conditions 2, see above).¹⁶ A (2.6 g, 6.4 mmol) was picolylated in toluene/NaOH_{aq} 50% (14 mL/10 mL) using 0.35 mL of *tert*-amyl alcohol, (NBu₄)⁺(HSO₄)⁻ (0.2 g, 0.1 eq.) and 2-picolyl chloride hydrochloride (2.5 g, 2.4 eq.). The product was purified by column chromatography (SiO₂, AcOEt–MeOH 95 : 5). Yield: 1.7 g (45%). ¹H NMR (360 MHz, CDCl₃): δ (ppm, see Scheme 3) 8.52 (d, 1H, $J = 5.0$ Hz, H_{6_{py}}), 8.46 (d, 1H, $J = 4.8$ Hz, H_{6_{py}}), 7.61 (td, 1H, $J_1 = 7.6, J_2 = 1.7$ Hz, H_{4_{py}a}), 7.47 (m, 7H, H_{4_{py}b}, 6 \times H_{tr}), 7.34 (d, 1H, $J = 7.8$ Hz, H_{3_{py}a}), 7.19 (m, 12H, H_{3_{py}b}, 2 \times H_{5_{py}}, 9 \times H_{tr}), 5.07 (d, 1H, $J = 3.5$ Hz, H1), 4.83 and 4.65 (2 \times d, 2 \times 1H, $J = 13.6$ Hz, 2 \times OCH₂Py), 4.46 (m, 1H, H4), 4.36 (quasi-t, $J_1 \approx J_2 = 4$ Hz, H3), 4.07 (m, 1H, H2), 3.57 (dd, $J_1 = 9.3$ Hz, $J_2 = 6.4$ Hz, H5a), 3.44 (s, 3H, Me), 3.38 (dd, $J_1 = 9.3$ Hz, $J_2 = 6.1$ Hz, H5b). ¹³C NMR (90 MHz, CDCl₃): δ (ppm) (158.5, 158.1) C_{2_{py}}, (148.8, 148.6) (C_{quatTr}), 144.0 C_{6_{py}}, (136.6, 136.5) C_{4_{py}}, (128.7, 127.7 and 127.9, C_{tr}), {122.3 (2C), 122.1, 121.1} (C_{3_{py}}, C_{5_{py}}), 106.5 C1, 84.3 C2, {(78.7 and 78.6) (C3, C4)}, (74.2, 73.4) CH₂-C_{2_{py}}, 62.7 C5, 56.0 Me.

Methyl 2,3-di-*O*-(2-picolyl)- α -D-lyxofuranoside (L1). B (1.7 g, 2.9 mmol) was dissolved in EtOH (95%) (50 mL). HCl aqueous solution (1M, 10 mL) was added and the resulting solution was stirred at ambient temperature overnight. Ethanol was evaporated. Water was added (*ca.* 70 mL) and the precipitate of triphenylcarbinol was filtered off. 60 mL of CHCl₃ was added to the aqueous solution that was then basified up to pH 11–12 by Na₂CO₃ and extracted twice further. The joined organic phases were dried on Na₂SO₄ and evaporated to provide an oil that was purified by column chromatography (SiO₂, AcOEt–MeOH, 9 : 1). Yield: 0.45 g (72%). Microanalysis (calc./found) C₁₈H₂₂N₂O₅·H₂O: C 59.33/59.25, H 6.08/6.12, N 7.69/7.71. ¹H NMR (360 MHz, CDCl₃): δ (ppm, see Scheme 3) 8.56 (d, 2H, $J = 4.8$ Hz, 2 \times H_{6_{py}}), 7.70 (m, 2H, 2 \times H_{4_{py}}), {7.50 (d, 1H, $J = 7.8$ Hz) and 7.30 (d, 1H, $J = 7.9$ Hz) 2 \times H_{3_{py}}}, 7.23 (m, 2H, 2 \times H_{5_{py}}), 5.10 (d, 1H, $J = 2.6$ Hz, H1), {4.94 (d, 1H, $J = 14.0$ Hz) and 4.8 (m, 3H), 2 \times OCH₂Py}, 4.44 (quasi-t, $J_1 \approx J_2 \approx 5$ Hz, H3), 4.36 (m, 1H, H4), 4.07 (dd, 1H, $J_1 = 4.6$ Hz, $J_2 = 2.6$ Hz, H2), 4.00 (dd, $J_1 = 11.4$ Hz, $J_2 = 7.3$ Hz, H5a), (dd, $J_1 = 11.4$ Hz, $J_2 = 4.61$ Hz, H5b), 3.41 (s, 3H, Me). ¹³C NMR (90 MHz, CDCl₃): δ (ppm) = (158.6, 158.0) C_{2_{py}}, (148.6, 148.5) C_{6_{py}}, (137.0, 136.7) C_{4_{py}}, {122.6, 122.3, 121.6 (2C) (C_{3_{py}}, C_{5_{py}})}, 99.5 C1, 83.1 C2, 79.2 C3, 78.7 C4, (73.9, 73.2) CH₂C_{2_{py}}, 60.5 C5, 55.6 Me. MS-ES: 369.2 (100%) [M + Na].

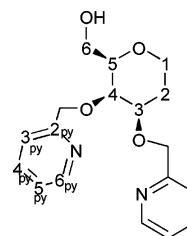


Scheme 3 Proton assignments.

1,5-Anhydro-2-deoxy-3,4-di-*O*-(2-picolyl)-6-*O*-trityl-D-galactitol (D). C (1,5-anhydro-2-deoxy-D-galactitol) was synthesized as previously published.¹⁷ C (1.5 g, 10.1 mmol) was tritylated on the 6-position by a conventional protocol using trityl chloride (3.7 g,

1.2 eq.) in pyridine (25 mL) at 50 °C with DMAP in catalytic amount. After one night, TLC analysis showed the disappearance of C. After addition of 2.5 mL water, the solvent was evaporated. CH₂Cl₂ (50 mL) was added and washed with water. The organic phases were dried on MgSO₄ anhydrous and evaporated to dryness. The 1,5-anhydro-2-deoxy-6-*O*-trityl-D-galactitol was purified by chromatography (SiO₂, from CH₂Cl₂ to CH₂Cl₂–MeOH, 95 : 5) and was used as such in the next step. It was then picolyated using an adaptation of a benzylation protocol by Szeja *et al.*¹⁶ (condition 1, see above) previously published.¹³ The picolylation was realized in toluene–DMSO (10 mL/2 mL) using 0.2 mL of *tert*-amyl alcohol, ground NaOH/K₂CO₃ (1.6 g/6.4 g), (NBu₄)⁺(HSO₄)⁻ (0.17 g, 0.1 eq.), and the solution of neutralized 2-picolyl chloride hydrochloride (2.1 g, 2.4 eq./1,5-anhydro-2-deoxy-6-*O*-trityl-D-galactitol). D was purified by column chromatography (SiO₂, elution gradient: AcOEt to AcOEt–MeOH 95 : 5). Yield: 1.73 g (56%). ¹H NMR (360 MHz, CDCl₃): δ (ppm, see Scheme 4) 8.45 (d, 1H, $J = 4.3$ Hz, H_{6_{py}a}), 8.34 (d, 1H, $J = 4.2$ Hz, H_{6_{py}b}), 7.70 (td, 1H, $J_1 = J_2 = 4.0$ Hz, H_{4_{py}a}), 7.47 (m, 7H, H_{4_{py}b}, 6 \times H_{tr}), 7.33 (d, 1H, $J = 12.6$ Hz, H_{3_{py}a}), 7.18 (m, 12H, H_{3_{py}b}, 2 \times H_{5_{py}}, 9 \times H_{tr}), {5.06 (d, 1H, $J = 13.7$ Hz), 4.92 (d, 1H, $J = 13.7$ Hz) OCH₂py}, {4.76 (d, 1H, $J = 13.4$ Hz), 4.72 (d, 1H, $J = 13.4$ Hz) OCH₂py}, 4.12 (m, 1H, H4), 4.08 (ddd, 1H, $J_1 = 1.5$ Hz, $J_2 = 4.6$ Hz, $J_3 = 11.4$ Hz, H1a), 3.92 (d, 2H, $J = 7.2$ Hz, H6), 3.72 (ddd, $J_1 = 2.5$ Hz, $J_2 = 4.3$ Hz, $J_3 = 11.7$ Hz, H3), {3.47 (m, 2H) H1b and H5}, 2.12 (qd, 1H, $J_1 \approx J_2 \approx J_3 \approx 12$ Hz, $J_4 = 4.6$ Hz, H2a), 1.95 (ddd, $J_1 = 1.61$ Hz, $J_2 = 4.2$ Hz, $J_3 = 12.5$ Hz, H2b). ¹³C NMR (90 MHz, CDCl₃): δ (ppm) (158.6, 158.4) C_{2_{py}}, (148.7, 148.5) C_{6_{py}}, 145.3 (C_{quatTr}), (137.5, 137.1) C_{4_{py}}, (129.4, 128.3, 128.6) C_{tr}, (122.9, 122.7, 122.4, 121.5) (C_{3_{py}}, C_{5_{py}}), 79.8 C3, 78.9 C5, 76.2 C4, (75.2, 71.5) CH₂C_{2_{py}}, 66.4 C1, 60.9 C6, 27.6 C2.

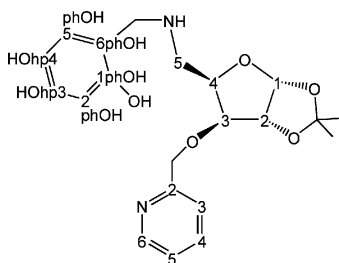
1,5-Anhydro-2-deoxy-3,4-di-*O*-(2-picolyl)-D-galactitol (L2). D (1.57 g, 2.7 mmol) was dissolved in EtOH (95%) (50 mL). HCl aqueous solution (1 M, 10 mL) was added and the resulting solution was stirred at ambient temperature overnight. Ethanol was evaporated. Water was added (60 mL) and the remaining precipitate of triphenylcarbinol was filtered off. 100 mL of CHCl₃ was added to the aqueous phase that was then basified up to pH 11–12 by Na₂CO₃ and extracted twice further. The joined organic phases were dried over Na₂SO₄ and evaporated to provide L2 as an oil. Yield 0.68 g (77%). Microanalysis (calc./found) C₁₈H₂₂N₂O₄·H₂O: C 62.05/61.91, H 6.36/6.46, N 8.04/7.98%. ¹H NMR (360 MHz, CDCl₃): δ (ppm, see Scheme 4) 8.57 (m, 2H, H_{6_{py}}), 7.70 (2H, m, H_{4_{py}}), 7.51 (d, $J = 7.8$ Hz, 1H, H_{3_{py}a}), {7.23 (m, 3H, $J = 7.9$ Hz) (H_{3_{py}b}, H_{5_{py}})}, {5.11 (d, 1H, $J = 13.8$ Hz), 4.93 (d, 1H, $J = 13.8$ Hz) OCH₂py}, {4.81 (d, 1H, $J = 13.5$ Hz), 4.75 (d, 1H, $J = 13.5$ Hz) OCH₂py}, 4.30 (m, 1H, H4), 4.09 (ddd, 1H, $J_1 = 1.6$ Hz, $J_2 = 4.8$ Hz, $J_3 = 11.5$ Hz, H1a), 3.76 (d, 2H,



Scheme 4 Proton assignments.

$J = 7.1$ Hz, H6), 3.70 (ddd, $J_1 = 2.6$ Hz, $J_2 = 4.5$ Hz, $J_3 = 11.8$ Hz, H3), 3.47 (m, 2H, H1b and H5), 2.22 (qd, 1H, $J_1 \approx J_2 \approx J_3 \approx 12$ Hz, $J_4 = 4.8$ Hz, H2a), 1.88 (ddd, $J_1 = 1.6$ Hz, $J_2 = 4.3$ Hz, $J_3 = 12.5$ Hz, H2b). ^{13}C NMR (92 MHz, CDCl_3): δ (ppm) (158.7, 158.6) $\text{C}_{2\text{py}}$, (149.1, 149.0) $\text{C}_{6\text{py}}$, (137.2, 136.7) $\text{C}_{4\text{py}}$, (122.8, 122.5, 122.3, 121.2) ($\text{C}_{3\text{py}}$, $\text{C}_{5\text{py}}$), 79.5 C3, 78.6 C5, 75.8 C4, (75.0, 71.3) $\text{CH}_2\text{C}_{2\text{py}}$, 66.2 C1, 60.4 C6, 27.2 C2. MS-ES: 331.2 (4%) [M + H]; 353.2 (100%) [M + Na].

5-Azido-5-deoxy-1,2-O-isopropylidene-3-O-(2-picolyl)- α -D-xylofuranose (F). 5-Azido-5-deoxy-1,2-O-isopropylidene- α -D-xylofuranose (E) was synthesized as previously published.¹⁷ The condition 2 were applied. E (1.29 g, 6 mmol) was picolyated in toluene/(NaOH_{aq} 50%) (14/10 mL) using 2-picolyl chloride hydrochloride (1.48 g, 9 mmol, 1.5 eq./E), 0.2 mL of *tert*-amyl alcohol, and NBu_4HSO_4 (0.19 g, 0.6 mmol, 0.1 eq.). After treatment (see above), F was purified by chromatography (SiO_2 , from CH_2Cl_2 to CH_2Cl_2 -MeOH, 9 : 1). Yield: 1.22 g (66%). Microanalysis: calc./found for $\text{C}_{14}\text{H}_{18}\text{N}_4\text{O}_4 \cdot 1/3\text{H}_2\text{O}$: C 54.10/54.06, H 6.00/5.78, N 17.94/17.69%. ^1H NMR (250 MHz, CDCl_3): δ (ppm, see Scheme 5) 8.53 (d, 1H, $J = 4.8$ Hz, $\text{H}_{6\text{py}}$), 7.69 (td, 1H, $J_1 = 7.7$ Hz, $J_2 = 1.6$ Hz, $\text{H}_{4\text{py}}$), 7.37 (d, 1H, $J = 7.7$ Hz, $\text{H}_{3\text{py}}$), 7.19 (m, 1H, $\text{H}_{5\text{py}}$), 5.92 (d, 1H, $J = 3.7$ Hz, H1), {4.78, (d, 1H, $J = 12.9$ Hz), 4.65 (m, 2H) OCH_2py , H2}, 4.32 (m, 1H, H4), 4.02 (d, $J = 3.1$ Hz, H3), 3.57 (m, 2H, $\text{H}_{5\text{a}}$ and $\text{H}_{5\text{b}}$), {1.48 and 1.30 ($2 \times \text{s}$, $2 \times 3\text{H}$, Me_{ip})}. ^{13}C NMR (62.5 MHz, CDCl_3): δ (ppm) 157.3 ($\text{C}_{2\text{py}}$), 149.2 ($\text{C}_{6\text{py}}$), 136.8 ($\text{C}_{4\text{py}}$), {122.8, 121.5} ($\text{C}_{3\text{py}}$, $\text{C}_{5\text{py}}$), 111.9 (C_{quatip}), 105.1 (C1), {82.2, 81.2} (C2, C4), 78.6 (C3), 72.6 (OCH_2py), 49.2 (C5), {26.8, 26.2} (Me_{ip}). MS-ES: 329.1 (100%) [M + Na].



Scheme 5 Proton assignments.

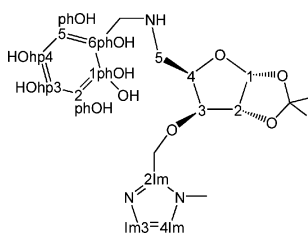
5-Amino-5-deoxy-1,2-O-isopropylidene-3-O-(2-picolyl)- α -D-xylofuranose (G). F (1 g, 3 mmol) was dissolved in MeOH (10 mL) and hydrogenated under pressure ($P(\text{H}_2) = 5$ bar) using Pd/C as a catalyst. After 3 h, the catalyst was removed by filtration on Celite which was washed with MeOH. The solvent was evaporated and G was obtained quantitatively as an oil. Microanalysis: calc./found for $\text{C}_{14}\text{H}_{20}\text{N}_2\text{O}_4 \cdot 2/3\text{H}_2\text{O}$: C 57.52/58.04, H 7.36/7.05, N 9.12/9.85%. ^1H NMR (250 MHz, CDCl_3): δ (ppm, see Scheme 5) 8.51 (m, 1H, $\text{H}_{6\text{py}}$), 7.65 (td, 1H, $J_1 = 7.7$ Hz, $J_2 = 1.7$ Hz, $\text{H}_{4\text{py}}$), 7.31 (d, 1H, $J = 7.7$ Hz, $\text{H}_{3\text{py}}$), 7.18 (m, 1H, $\text{H}_{5\text{py}}$), 5.90 (d, 1H, $J = 3.7$ Hz, H1), {4.77 and 4.59 ($2 \times \text{d}$, $2 \times 1\text{H}$, $J = 13.3$ Hz, OCH_2py)}, 4.63 (d, $J = 3.7$ Hz, H2), 4.24 (m, 1H, H4); 4.00 (d, $J = 3.2$ Hz, H3), 3.07 (m, 2H, $\text{H}_{5\text{a}}$ and $\text{H}_{5\text{b}}$), {1.44 and 1.26 ($2 \times \text{s}$, $2 \times 3\text{H}$, Me_{ip})}. ^{13}C NMR (62.5 MHz, CDCl_3): δ (ppm) 157.0 ($\text{C}_{2\text{py}}$), 149.0 ($\text{C}_{6\text{py}}$), 137.1 ($\text{C}_{4\text{py}}$), {122.9, 121.5} ($\text{C}_{3\text{py}}$, $\text{C}_{5\text{py}}$), 111.7 (C_{quatip}), 104.9 (C1), {82.8, 82.1} (C2, C4), 80.3 (C3), 72.0

(OCH_2py), 40.0 (C5), {26.7 and 26.2 (Me_{ip})}. MS-ES: 281.2 (5%) [M + H]; 303.1 (100%) [M + Na].

5-(Amino-N-(2-salicyl))-5-deoxy-1,2-O-isopropylidene-3-O-(2-picolyl)- α -D-xylofuranose (L3). G (500 mg, 1.78 mmol, 1 eq.) was dissolved in 15 mL absolute ethanol. Salicylaldehyde (217 mg, 1.78 mmol, 1 eq.) was added, which caused the immediate appearance of a yellow colour. The solution was cooled (water-ice bath), NaBH_4 (67 mg, 1.77 mmol, 1 eq.) was added inducing the disappearance of the yellow coloration. The reaction mixture was stirred more than 30 minutes at RT. Excess NaBH_4 was destroyed with acetic acid. The solvent was evaporated and L3 was purified by chromatography (AcOEt -MeOH/ NH_3 , v/v/v = 95/5/2). Yield: 420 mg (61%). Microanalysis (calc./found) $\text{C}_{21}\text{H}_{26}\text{N}_2\text{O}_5 \cdot 0.4\text{H}_2\text{O}$: C 64.07/64.12, H 6.86/6.81, N 7.12/6.35%. ^1H NMR (300 MHz, CDCl_3): δ (ppm, see Scheme 5) 8.30 (1H, d, $J = 4.3$ Hz, $\text{H}_{6\text{py}}$), 7.61 (1H, td, $J_1 = 7.7$ Hz, $J_2 = 1.6$ Hz, $\text{H}_{4\text{py}}$), 7.24 (1H, d, $J = 7.7$ Hz, $\text{H}_{3\text{py}}$), {7.12 (m, 2H), 6.96 (d, 1H, $J = 6.6$ Hz), 6.77 (m, 2H), (H_{PhOH} s, $\text{H}_{5\text{py}}$)}, 5.92 (d, 1H, $J = 3.8$ Hz, H1), {4.76 and 4.58 ($2 \times \text{d}$, $2 \times 1\text{H}$, $J = 13.4$ Hz, OCH_2py)}, 4.65 (d, 1H, $J = 3.8$ Hz, H2), 4.37 (td, $J_1 = 7.0$ Hz, $J_2 = 3.3$ Hz, H4), {4.05 and 3.92 ($2 \times \text{d}$, $2 \times 1\text{H}$, $J = 13.9$ Hz, NHCH_2PhOH)}, 3.9 (d, $J = 3.3$ Hz, H3), 2.98 (m, 2H, $\text{H}_{5\text{a}}$, $\text{H}_{5\text{b}}$), {1.47 and 1.30 ($2 \times \text{s}$, $2 \times 3\text{H}$, Me_{ip})}. ^{13}C NMR (75 MHz, CDCl_3): δ (ppm) {158.2 and 157.1 ($\text{C}_{1\text{PhOH}}$ and $\text{C}_{2\text{py}}$)}, 149.1 ($\text{C}_{6\text{py}}$), 136.8 ($\text{C}_{4\text{py}}$), {128.7, 128.5, 122.8, and 121.6 ($\text{C}_{3\text{py}}$, $\text{C}_{5\text{py}}$, $\text{C}_{3\text{PhOH}}$, $\text{C}_{5\text{PhOH}}$)}, 126.1 ($\text{C}_{2\text{PhOH}}$), {119.0 and 116.3, ($\text{C}_{6\text{PhOH}}$, $\text{C}_{4\text{PhOH}}$)}, 111.7 (C_{quatip}), 104.9 (C1), {82.4 and 82.1 (C2, C4)}, 78.8 (C3), 71.8 (OCH_2Py), 52.6 (NHCH_2PhOH), 48.6 (C5), {26.7 and 26.2 (Me_{ip})}. MS-ES: 409.2 (100%) [M + Na].

5-Azido-5-deoxy-1,2-O-isopropylidene-3-O-(N-methylimidazol-2-yl)- α -D-xylofuranose (H). H was synthesized using the same protocol as F using 2-imidazolyl chloride hydrochloride⁴² instead of 2-picolyl chloride hydrochloride and E. E (1.84 g, 8.55 mmol) was imidazolated in toluene/(NaOH_{aq} 50%) (14/10 mL) using 2-imidazolyl chloride hydrochloride (1.71 g, 10.26 mmol, 1.2 eq./E), 0.35 mL of *tert*-amyl alcohol and NBu_4HSO_4 (0.28 g, 0.85 mmol, 0.1 eq.). After treatment (see above), H was purified by chromatography (SiO_2 , elution gradient: AcOEt to AcOEt -MeOH 95 : 5). Yield: 1.50 g (57%). ^1H NMR (250 MHz, CDCl_3): δ (ppm, see Scheme 6) 6.73 (1H, d, $J = 6.9$ Hz, $\text{H}_{3\text{im}}$), 6.70 (1H, d, $J = 6.9$ Hz, $\text{H}_{4\text{im}}$), 5.64 (1H, d, $J = 3.6$ Hz, H1), {4.49 (d, 1H, $J = 12.4$ Hz), 4.46 (m, 2H) (OCH_2Im , H2)}, 4.33 (m, 1H, H4), 4.06 (d, $J = 2.9$ Hz, H3), 3.46 (s, 3H, Me_{im}), 3.26 (dd, $J_1 = 12.0$ Hz, $J_2 = 7.4$ Hz, $\text{H}_{5\text{a}}$), 3.11 (dd, $J_1 = 12.0$ Hz, $J_2 = 4.8$ Hz, $\text{H}_{5\text{b}}$), {1.25 and 1.08 ($2 \times \text{s}$, $2 \times 3\text{H}$, Me_{ip})}. ^{13}C NMR (90 MHz, CDCl_3): δ (ppm) 143.4 ($\text{C}_{2\text{im}}$), 127.5 ($\text{C}_{3\text{im}}$), 122.2, ($\text{C}_{4\text{im}}$), 111.7 (C_{quatip}), 104.8 (C1), {(81.6, 81.1, 78.3) (C2, C3, C4)}, 63.2 (OCH_2Im), 48.9 (C5), 32.6 (Me_{im}), (26.5, 26.0) (OCMe_2).

5-Amino-5-deoxy-1,2-O-isopropylidene-3-O-(N-methylimidazol-2-yl)- α -D-xylofuranose (I). I was synthesized quantitatively using the same protocol as G. H (0.88 g, 2.84 mmol) was dissolved in MeOH (10 mL) and hydrogenated under pressure ($P(\text{H}_2) = 5$ bar) using Pd/C as a catalyst. After one night, the catalyst was removed by filtration on Celite which was washed with MeOH. The solvent was evaporated and I was obtained quantitatively as an oil. ^1H NMR (250 MHz, CDCl_3): δ (ppm, see Scheme 6) 6.83 (1H, d, $J = 7.0$ Hz, $\text{H}_{3\text{im}}$), 6.78 (1H, d, $J = 7.1$ Hz, $\text{H}_{4\text{im}}$), 5.85 (1H, d, $J = 3.8$ Hz, H1), {4.62 (d, 1H, $J = 12.6$ Hz),



Scheme 6 Proton assignments.

4.58 (m, 2H) (OCH_2Im , H2)}, 4.29 (m, 1H, H4), 3.94 (d, $J = 2.9$ Hz, H3), 3.53 (s, 3H, Me_{Im}), 2.84 (dd, $J_1 = 12.1$ Hz, $J_2 = 7.5$ Hz, H5a), 2.69 (dd, $J_1 = 12.1$ Hz, $J_2 = 4.9$ Hz, H5b), {1.44 and 1.25 ($2 \times s$, $2 \times 3\text{H}$, Me_{IP})}. ^{13}C NMR (90 MHz, CDCl_3): δ (ppm) 143.6 ($\text{C}_{2\text{Im}}$), 127.9 ($\text{C}_{3\text{Im}}$), 122.7, ($\text{C}_{4\text{Im}}$), 111.7 ($\text{C}_{\text{quat IP}}$), 104.9 (C1), (82.6, 81.9, 78.9) (C2, C3, C4), 63.1 (OCH_2Im), 52.4 (C5), 32.7 (Me_{Im}), (26.8, 26.1) (OCMe_2).

5-(Amino-*N*-(2-salicyl))-5-deoxy-1,2-*O*-isopropylidene-3-*O*-(methylimidazol-2-yl)- α -D-xylofuranose (L4**).** **L4** was synthesized using the same protocol as **L3**. **I** (600 mg, 2.12 mmol, 1 eq.) was dissolved in 15 mL absolute ethanol. Salicylaldehyde (694 mg, 5.68 mmol, 2 eq.) was added which caused the immediate appearance of a yellow colour. The solution was cooled (water-ice bath). NaBH_4 (61.1 mg, 2.12 mmol, 1 eq.) was added inducing a disappearance of the yellow coloration. The reaction mixture was then stirred for 30 min at RT. Excess NaBH_4 was destroyed with acetic acid. The solvent was evaporated and **L4** was purified by chromatography (AcOEt-MeOH-NH_3 , $v/v/v = 95/5/2$). Yield: 560 mg (68%). Microanalysis (calc./found) $\text{C}_{20}\text{H}_{27}\text{N}_3\text{O}_5 \cdot \text{H}_2\text{O}$: C 58.96/59.01, H 6.68/6.72, N 10.31/10.29%. ^1H NMR (360 MHz, CDCl_3): δ (ppm, see Scheme 6) 7.07 (1H, t, $J = 7.6$ Hz, $\text{H}_{3\text{PhOH}}$), {6.90 (1H, d, $J = 7.2$ Hz), 6.7 (2H, m) ($\text{H}_{2\text{PhOH}}$, $\text{H}_{4\text{PhOH}}$, $\text{H}_{5\text{PhOH}}$)}, 6.79 (1H, s_{large} , $\text{H}_{3\text{Im}}$), 6.74 (1H, s_{large} , $\text{H}_{4\text{Im}}$), 5.80 (1H, d, $J = 3.7$ Hz, H1), {4.60 (d, 1H, $J = 12.8$ Hz), 4.5 (m, 2H) (OCH_2Im , H2)} 4.24 (m, 1H, H4), 3.95 (d, 1H, $J = 13.8$ Hz, $\text{NHCH}_{2a}\text{PhOH}$), 3.90 (d, $J = 3.0$ Hz, H3), 3.81 (d, 1H, $J = 13.8$ Hz, $\text{NHCH}_{2b}\text{PhOH}$), 3.49 (s, 3H, Me_{Im}), 2.82 (dd, $J_1 = 12.3$ Hz, $J_2 = 7.6$ Hz, H5a), 2.67 (dd, $J_1 = 12.3$ Hz, $J_2 = 5.0$ Hz, H5b), {1.40 and 1.23 ($2 \times s$, $2 \times 3\text{H}$, Me_{IP})}. ^{13}C NMR (90 MHz, CDCl_3): 143.6 ($\text{C}_{2\text{Im}}$), {(128.6, 128.5, 127.5) ($\text{C}_{3\text{PhOH}}$, $\text{C}_{5\text{PhOH}}$, $\text{C}_{3\text{Im}}$)}, {(122.2, 118.9, 116.2) ($\text{C}_{4\text{Im}}$, $\text{C}_{2\text{PhOH}}$, $\text{C}_{4\text{PhOH}}$)}, 111.7 ($\text{C}_{\text{quat IP}}$), 104.5 (C1), {(82.1, 81.8, 78.7) (C2, C3, C4)}, 63.2 (OCH_2Im), 52.4 ($\text{NH-CH}_2\text{-PhOH}$), 46.4 (C5), 32.7 (Me_{Im}), (26.7, 26.1) (OCMe_2). MS-ES: 389.2 (23%) [M]; 388.2 (100%) [M – H].

Copper complexes [$\text{Cu}^{\text{I}}(\text{Ln})$]

The protocol was the same for all the complexes. The synthesis of $\text{Cu}^{\text{I}}\text{L1}$ is detailed here. Degassed methanol solutions (1 mL) of methyl-2,3-di-*O*-(2-picolyl)- α -D-lyxofuranoside (**L1**, 20 mg, 0.0577 mmol) and $[\text{Cu}(\text{CH}_3\text{CN})_4][\text{PF}_6]$ (21.5 mg, 0.0577 mmol) were separately prepared under Ar in a glove box. The copper(I) salt solution was added dropwise to the ligand solution, and the resulting bright yellow solution was stirred during a few minutes. Slow evaporation led to a colourless solid.

Characterization of $\text{Cu}^{\text{I}}\text{L1}$. Yield: 22 mg (0.054 mmol, 93%). IR (KBr): $\nu(\text{cm}^{-1})$ 1615 ($\nu\text{C}=\text{N}$), 1574 ($\nu\text{C}=\text{C}$). Anal. Calc. for $\text{C}_{18}\text{H}_{22}\text{N}_2\text{O}_5\text{CuPF}_6 \cdot \text{H}_2\text{O}$: C, 37.73; H, 4.19; N, 4.89; Cu, 11.09.

Found: C, 37.65; H, 4.09; N, 5.06; Cu, 11.19%. HR-MS: m/z (%): 409.0823 (100) (calc m/z for $\text{C}_{18}\text{H}_{22}\text{N}_2\text{O}_5\text{Cu}$ 409.0819 [$\text{Cu}^{\text{I}}\text{L}^+$]).

Characterization of $\text{Cu}^{\text{I}}\text{L2}$. Yield: 22 mg (0.056 mmol, 92%). IR (KBr): $\nu(\text{cm}^{-1})$ 1610 ($\nu\text{C}=\text{N}$), 1572 ($\nu\text{C}=\text{C}$). Anal. Calc. for $\text{C}_{18}\text{H}_{22}\text{N}_2\text{O}_4\text{CuPF}_6 \cdot \text{H}_2\text{O}$: C, 38.82; H, 4.34; N, 5.04; Cu, 11.41. Found: C, 38.61; H, 4.35; N, 5.24; Cu, 11.48%. HR-MS: m/z (%): 393.0875 (100) (calc. m/z for $\text{C}_{18}\text{H}_{22}\text{N}_2\text{O}_4\text{Cu}$ 393.0825 [$\text{Cu}^{\text{I}}\text{L}^+$]).

Characterization of $\text{Cu}^{\text{I}}\text{L3}$. Yield: 23 mg (0.051 mmol, 91%). IR (KBr): $\nu(\text{cm}^{-1})$ 1615 ($\nu\text{C}=\text{N}$), 1568 ($\nu\text{C}=\text{C}$). Anal. Calc. for $\text{C}_{21}\text{H}_{26}\text{N}_2\text{O}_5\text{CuPF}_6 \cdot \text{H}_2\text{O}$: C, 41.14; H, 4.24; N, 4.57; Cu, 10.37. Found: C, 40.98; H, 4.04 N, 4.73; Cu, 9.66%. HR-MS: m/z (%): 448.0957 (100) (calc. m/z for $\text{C}_{21}\text{H}_{25}\text{N}_2\text{O}_5\text{Cu}$ 448.1123 [$\text{Cu}^{\text{II}}\text{L}^+$]).

Characterization of $\text{Cu}^{\text{I}}\text{L4}$. Yield: 21 mg (0.046 mmol, 91%). IR (KBr): $\nu(\text{cm}^{-1})$ 1614 ($\nu\text{C}=\text{N}$), 1572 ($\nu\text{C}=\text{C}$). Anal. Calc. for $\text{C}_{20}\text{H}_{27}\text{N}_3\text{O}_5\text{CuPF}_6 \cdot \text{H}_2\text{O}$: C, 38.99; H, 4.39; N, 6.82; Cu, 10.32. Found: C, 39.38; H, 4.68; N, 6.77; Cu, 10.79%. HR-MS: m/z (%): 451.1160 (100) (calc. m/z for $\text{C}_{20}\text{H}_{26}\text{N}_3\text{O}_5\text{Cu}$ 451.1163 [$\text{Cu}^{\text{II}}\text{L}^+$]).

The copper(I) complexes ($\text{Cu}^{\text{I}}\text{L3}$ and $\text{Cu}^{\text{I}}\text{L4}$) are oxidized in the spray and detected as adducts of copper(II) complexes, which differ by one mass units only, due to the deprotonation of the phenolic moiety coordinated to the metallic centre induced by its oxidation.

Acknowledgements

We thank the Région Champagne-Ardenne for a grant to Z. D. and for its financial support, and the French ministry government for financial support (ACI-jeune chercheurs JC4044) for C. P. The C.R.I.H.A.N computing center (<http://www.crihan.fr>) and the computational center of the Université de Reims Champagne-Ardenne (ROMEO: <http://www.romeo2.univ-reims.fr>) are acknowledged for the CPU time donated.

References

- J. P. Klinman, *Chem. Rev.*, 1996, **96**, 2541.
- E. I. Solomon, U. M. Sundaram and T. E. Machonkin, *Chem. Rev.*, 1996, **96**, 2563.
- N. Kitajima and Y. Moro-Oka, *Chem. Rev.*, 1994, **94**, 737.
- K. D. Karlin and Z. Tyeklar, *Bioinorganic Chemistry of Copper*, Chapman & Hall, New-York, 1993.
- D. H. Lee, L. Q. Hatcher, M. A. Vance, R. Sarangi, A. E. Milligan, A. A. Narducci, Sarjeant, C. D. Incarvito, A. L. Rheingold, K. O. Hodgson, B. Hedman, E. I. Solomon and K. D. Karlin, *Inorg. Chem.*, 2007, **46**, 6056.
- L. M. Mirica, X. Ottenwaelder and T. D. P. Stack, *Chem. Rev.*, 2004, **104**, 1013.
- E. A. Lewis and W. B. Tolman, *Chem. Rev.*, 2004, **104**, 1047.
- J. Miltz and M. Perry, *Packag. Technol. Sci.*, 2005, **18**, 21.
- P. Cook, Stealth scavenging systems: the scavenger in the polymer, in *International Food Technologists Annual Meeting Book of Abstracts*, IFT, Atlanta, GA, 1998.
- M. L. Rooney, Overview of oxygen-scavenging technologies, in *International Food Technologists Annual Meeting Book of Abstracts*, IFT, New Orleans, LA, 2001.
- G. Tewari, D. S. Jayas, L. E. Jeremiah and R. A. Holley, *Int. J. Food Sci. Technol.*, 2002, **37**, 209.
- F. Bellot, R. Hardré, G. Pelosi, M. Thérèsod and C. Polcar, *Chem. Commun.*, 2005, 5414.
- F. Cisnetti, R. Guillot, M. Desmadril, G. Pelosi and C. Polcar, *Dalton Trans.*, 2007, 1473.
- G. Charron, F. Bellot, F. Cisnetti, G. Pelosi, J.-N. Rebilly, E. Rivière, A.-L. Barra, T. Mallah and C. Polcar, *Chem.-Eur. J.*, 2007, **13**, 2774.

- 15 F. Cisnetti, R. Guillot, M. Thérissod and C. Policar, *Acta Crystallogr., Sect. C: Cryst. Struct. Commun.*, 2007, **63**, m201.
- 16 W. Szeja, I. Fokt and G. Gryniewicz, *Recl. Trav. Chim. Pays-Bas*, 1989, **108**, 224.
- 17 S. Hotha, R. I. Aneundi and A. A. Natu, *Tetrahedron Lett.*, 2005, **46**, 4585.
- 18 S. Miertus, E. Scrocco and J. Tomasi, *Chem. Phys.*, 1981, **55**, 117.
- 19 M. Cossi, G. Scalmani, N. Rega and V. Barone, *J. Chem. Phys.*, 2002, **117**, 43.
- 20 R. Cammi, B. Mennucci and J. Tomasi, *J. Phys. Chem. A*, 2000, **104**, 5631.
- 21 N. G. Connelly and W. E. Geiger, *Chem. Rev.*, 1996, **96**, 877.
- 22 L. Q. Hatcher, M. A. Vance, A. A. Narducci, Sarjeant, E. I. Solomon and K. D. Karlin, *Inorg. Chem.*, 2006, **45**, 3004.
- 23 P. Winget, E. J. Weber, C. J. Cramer and D. G. Truhlar, *Phys. Chem. Chem. Phys.*, 2000, **2**, 1231.
- 24 H. Kunkely and A. Vogler, *Inorg. Chim. Acta*, 2004, **357**, 888.
- 25 A. B. P. Lever, *Inorganic Electronic Spectroscopy*, Elsevier, New York, 1984.
- 26 J. Peisach and W. E. Blumberg, *Arch. Biochem. Biophys.*, 1974, **165**, 691.
- 27 P. J. Benites, D. S. Rawat and J. M. Zaleski, *J. Am. Chem. Soc.*, 2000, **122**, 7208.
- 28 B. J. Hathaway and D. E. Billing, *Coord. Chem. Rev.*, 1970, **5**, 143.
- 29 I. Bertini, D. Gatteschi and A. Scozzafava, *Inorg. Chem.*, 1977, **16**, 1973.
- 30 G. F. Kokoszka, C. W. Reimann and H. C. Allen, *J. Phys. Chem.*, 1967, **71**, 121.
- 31 M. J. Frisch, G. W. Trucks, H. B. Schlegel, G. E. Scuseria, M. A. Robb, J. R. Cheeseman, J. A. Montgomery, Jr., T. Vreven, K. N. Kudin, J. C. Burant, J. M. Millam, S. S. Iyengar, J. Tomasi, V. Barone, B. Mennucci, M. Cossi, G. Scalmani, N. Rega, G. A. Petersson, H. Nakatsuji, M. Hada, M. Ehara, K. Toyota, R. Fukuda, J. Hasegawa, M. Ishida, T. Nakajima, Y. Honda, O. Kitao, H. Nakai, M. Klene, X. Li, J. E. Knox, H. P. Hratchian, J. B. Cross, V. Bakken, C. Adamo, J. Jaramillo, R. Gomperts, R. E. Stratmann, O. Yazyev, A. J. Austin, R. Cammi, C. Pomelli, J. Ochterski, P. Y. Ayala, K. Morokuma, G. A. Voth, P. Salvador, J. J. Dannenberg, V. G. Zakrzewski, S. Dapprich, A. D. Daniels, M. C. Strain, O. Farkas, D. K. Malick, A. D. Rabuck, K. Raghavachari, J. B. Foresman, J. V. Ortiz, Q. Cui, A. G. Baboul, S. Clifford, J. Cioslowski, B. B. Stefanov, G. Liu, A. Liashenko, P. Piskorz, I. Komaromi, R. L. Martin, D. J. Fox, T. Keith, M. A. Al-Laham, C. Y. Peng, A. Nanayakkara, M. Challacombe, P. M. W. Gill, B. G. Johnson, W. Chen, M. W. Wong, C. Gonzalez and J. A. Pople, *GAUSSIAN 03 (Revision D.02)*, Gaussian, Inc., Wallingford, CT, 2004.
- 32 I. Morao, J. P. McNamara and I. H. Hillier, *J. Am. Chem. Soc.*, 2003, **125**, 628.
- 33 M. Itagaki, K. Masumoto, K. Suenobu and Y. Yamamoto, *Org. Process Res. Dev.*, 2006, **10**, 245.
- 34 J. Cody, J. Dennisson, J. Gilmore, D. G. VanDerveer, M. M. Henary, A. Gabrielli, C. D. Sherrill, Y. Zhang, C.-P. Pan, C. Burda and C. J. Fahrni, *Inorg. Chem.*, 2003, **42**, 4918.
- 35 C. Lee, W. Yang and R. G. Parr, *Phys. Rev. B: Condens. Matter Mater. Phys.*, 1988, **37**, 785.
- 36 B. Miehlich, A. Savin, H. Stoll and H. Preuss, *Chem. Phys. Lett.*, 1989, **157**, 200.
- 37 S. H. Vosko, L. Wilk and M. Nusair, *Can. J. Phys.*, 1980, **58**, 1200.
- 38 A. D. Becke, *J. Chem. Phys.*, 1993, **98**, 5648.
- 39 G. Schaftenaar and J. H. Noordik, *J. Comput. Aided Mol. Des.*, 2000, **14**, 123.
- 40 W. Humphrey, A. Dalke and K. Schulten, *J. Mol. Graphics*, 1996, **14**, 33.
- 41 W. G. Overend, F. Shafizadeh and M. Stacey, *J. Chem. Soc.*, 1950, 671.
- 42 P. Gamez, C. Simons, G. Aromi, W. L. Driessen, G. Challa and J. Reedijk, *J. Appl. Catal. A: General*, 2001, **214**, 187.